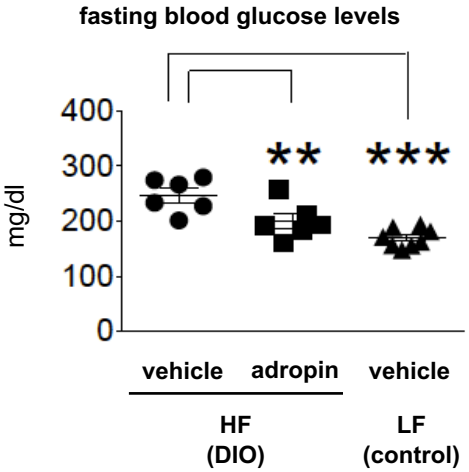
fasting blood glucose levels
mg/dl
400
300
200
100
0
**
***
vehicle
adropin
vehicle
HF
(DIO)
LF
(control)

Supp. Fig. 1

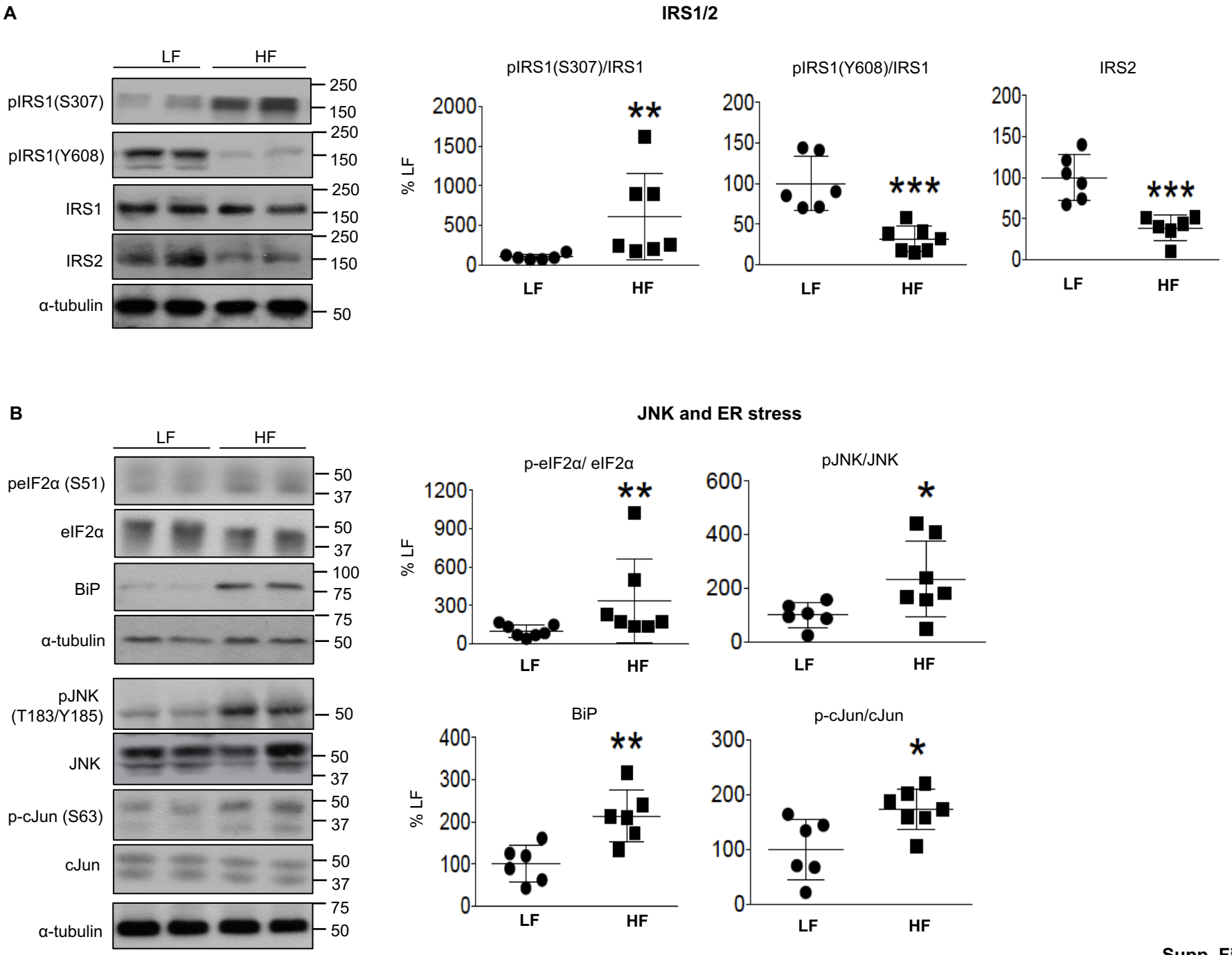
A
IRS1/2
LF
HF
pIRS1(S307)
pIRS1(Y608)
IRS1
IRS2
α-tubulin
250
150
50
pIRS1(S307)/IRS1
pIRS1(Y608)/IRS1
IRS2
% LF
2000
1500
1000
500
0
200
150
100
50
**
***
B
JNK and ER stress
peIF2α (S51)
eIF2α
BiP
α-tubulin
pJNK (T183/Y185)
JNK
p-cJun (S63)
cJun
100
75
37
p-eIF2α/ eIF2α
pJNK/JNK
BiP
p-cJun/cJun
1200
900
600
300
400
*

Supp. Fig. 2

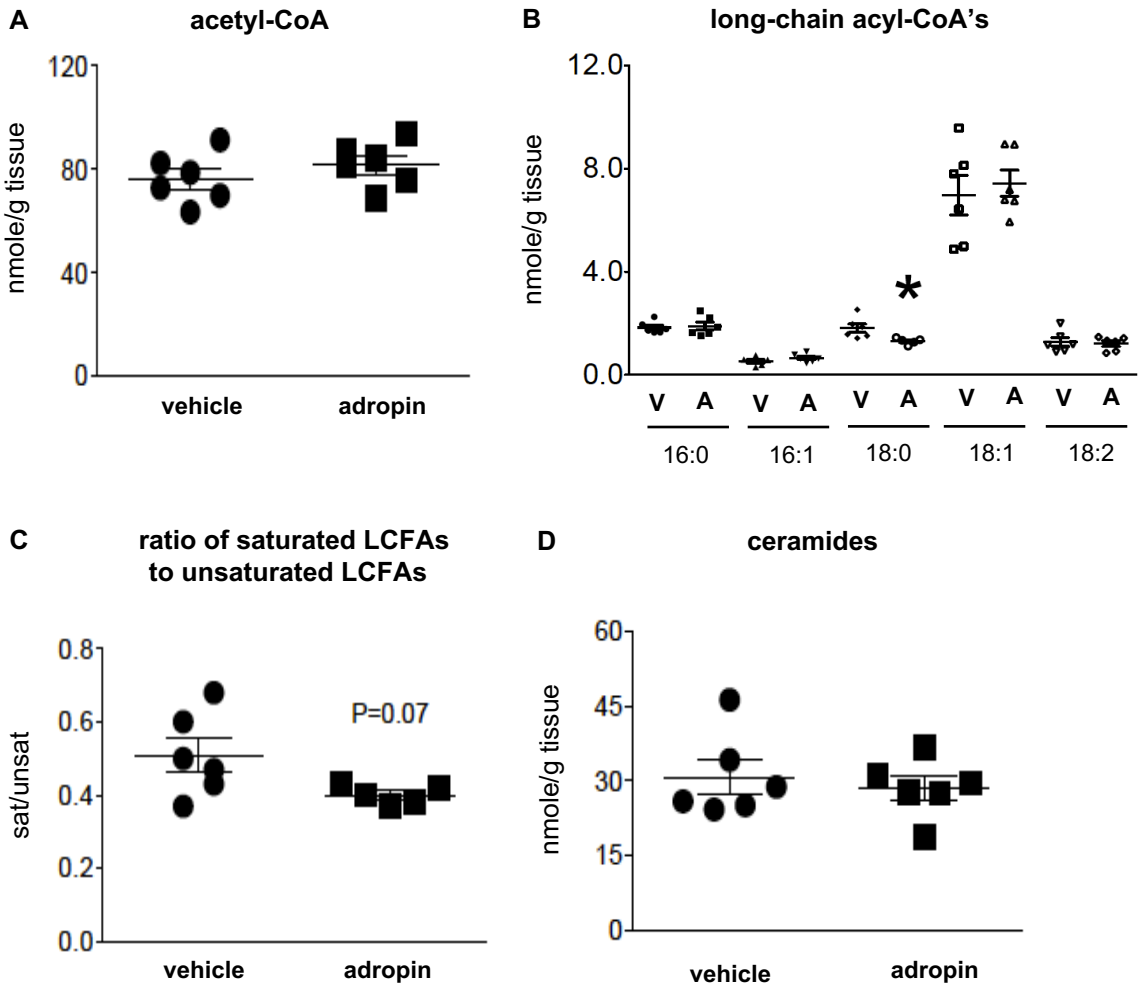
A
acetyl-CoA
nmole/g tissue
120
80
40
0
vehicle
adropin
B
long-chain acyl-CoA's
nmole/g tissue
12.0
8.0
4.0
0.0
*
V A V A V A V A V A
16:0 16:1 18:0 18:1 18:2
C
ratio of saturated LCFAs
to unsaturated LCFAs
sat/unsat
0.8
0.6
0.4
0.2
0.0
P=0.07
vehicle
adropin
D
ceramides
nmole/g tissue
60
45
30
15
0
vehicle
adropin

Supp. Fig. 3

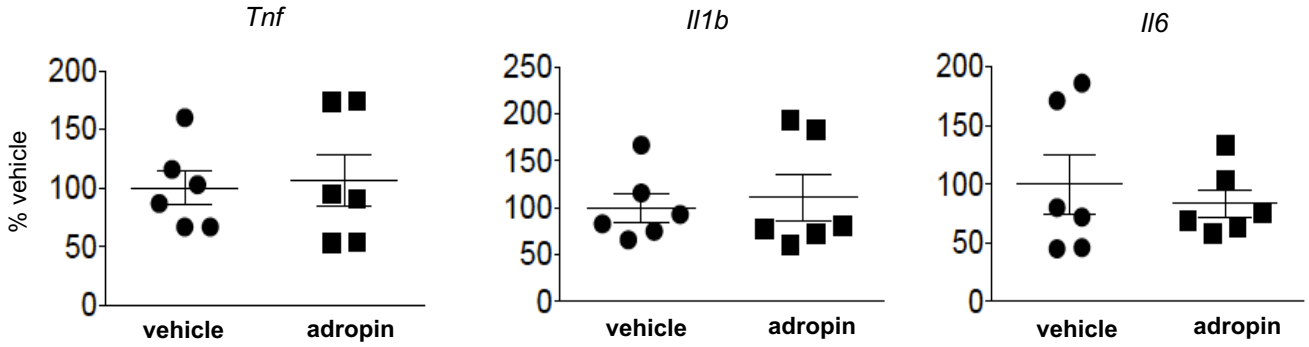
Tnf
Il1b
Il6
% vehicle
200
150
100
50
0
250
200
150
100
50
0
200
150
100
50
0
vehicle
adropin
vehicle
adropin
vehicle
adropin

Supp. Fig. 4

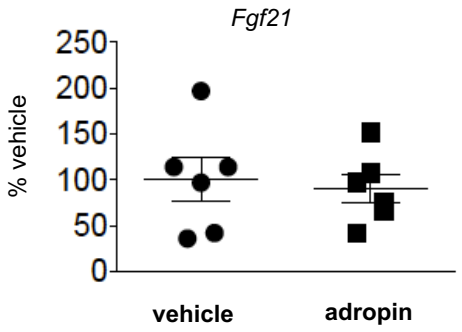

Supp. Fig. 5

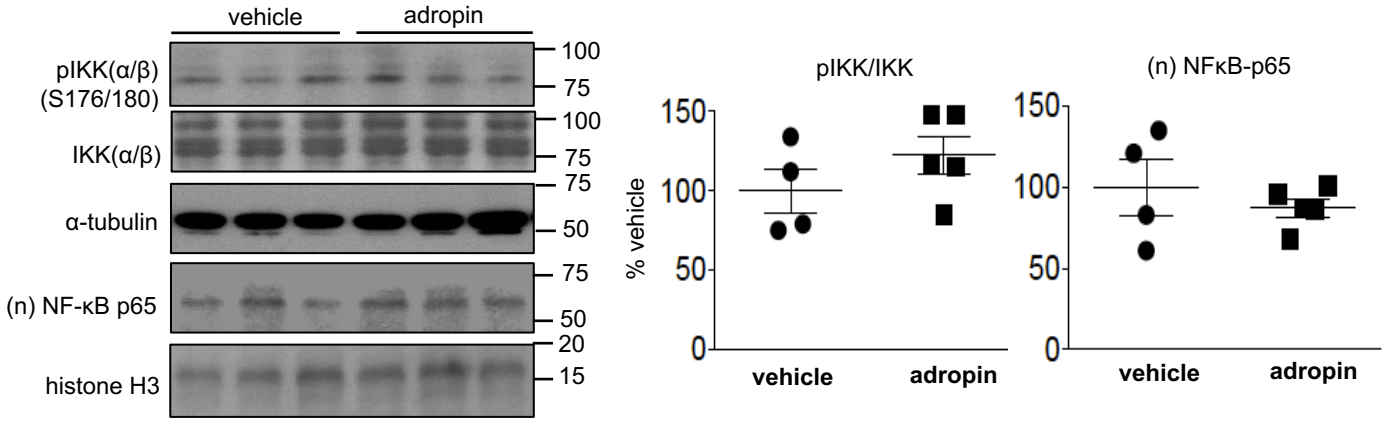
vehicle
adropin
pIKK(α/β)
(S176/180)
IKK(α/β)
α-tubulin
(n) NF-κB p65
histone H3
100
75
100
75
75
50
75
50
20
15
pIKK/IKK
(n) NFκB-p65
% vehicle
150
100
50
0
vehicle
adropin

Supp. Fig. 6

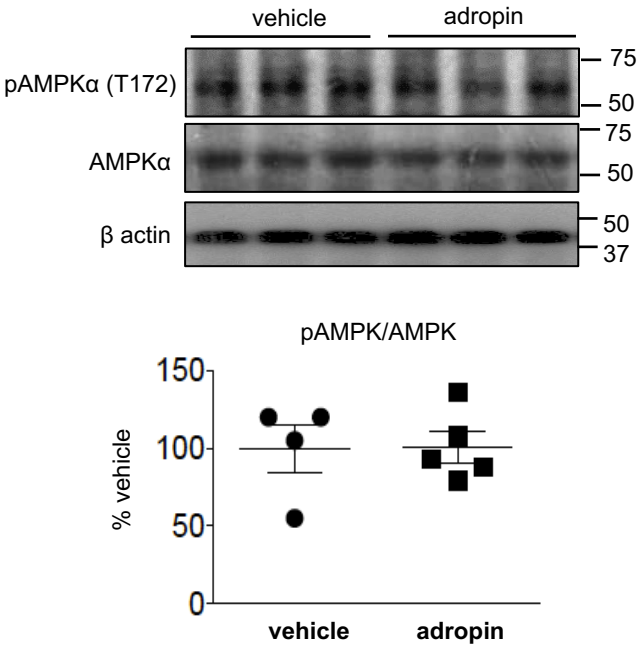
vehicle
adropin
pAMPKα (T172)
AMPKα
β actin
75
50
75
50
50
37
pAMPK/AMPK
% vehicle
150
100
50
0
vehicle
adropin

Supp. Fig. 7

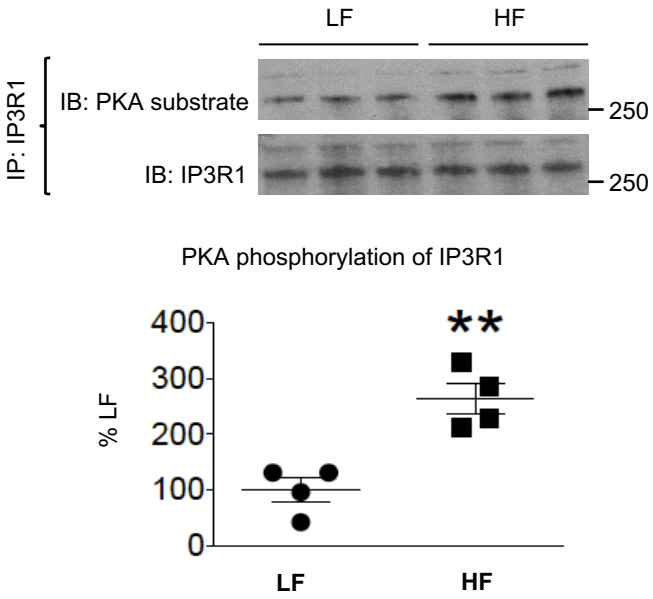
LF
HF
IP: IP3R1
IB: PKA substrate
250
IB: IP3R1
250
PKA phosphorylation of IP3R1
400
300
200
100
0
% LF
**
LF
HF

Supp. Fig. 8

Supplementary figure legends

S1 Adropin$^{34-76}$ treatment reduced blood glucose level in 6h-fasted DIO mice.

Diet-induced obese (DIO) mice maintained on high fat diet (HF) and lean mice (control) maintained on low fat diet (LF) received 5 injections of adropin$^{34-76}$ or vehicle. HF/veh: n=6, HF/adr: n=6, LF/veh: n=8. Six-hour fasting period encompassed 5h before and 1h after the last injection. One hour after the last injection, tail blood glucose levels were determined.

S2 Diet-induced obese mice displayed altered IRS signaling, increased JNK activity and ER stress responses in the liver.

DIO mice were maintained on high fat diet (HF), and lean mice maintained on low fat diet (LF) were used as the control. (A) The phosphorylation levels of Ser-307 in IRS1 (n=6-7) and Tyr 608 in IRS1(n=6-7) as well as total IRS2 protein levels (n=6) were determined by Western blotting. HF vs LF: **, $P<0.01$; ***, $P<0.0005$. (B) The phosphorylation levels of Ser51 in eIF2α (n=7), BiP protein levels (n=6), the phosphorylation levels of Thr-183/Tyr--185 in JNK (n=6-7) and the phosphorylation levels of Ser63 in c-Jun (n=6-7) were determined by Western blotting. α-tubulin was used as the loading control.

S3 Adropin$^{34-76}$ treatment did not exert major effects on the levels of fatty acid metabolites in the liver.

Lipidomics was performed to quantify the levels of acetyl-CoA (A, n=6), individual long-chain acyl-CoA's (B, n=5-6), the ratio of saturated fatty acyl-CoA levels (16:0 plus 18:0)

to unsaturated fatty acyl-CoA levels (16:1 plus 18:1) (C, n=5-6) and ceramides (D, n=6). adropin vs vehicle: *, $P \leq 0.05$.

S4 Adropin$^{34-76}$ treatment did not alter the expressions of inflammatory cytokines in the liver.

The message levels of inflammatory cytokines including tumor necrosis factor (*Tnf)*, interleukin-1b (*Il1b*) and interleukin-6 (*Il6*) were determined by real-time RT-PCR (n=6).

S5 Adropin$^{34-76}$ treatment did not alter the expression of FGF21 in the liver.

The message levels of fibroblast growth factor 21(*Fgf21*) was determined by real-time RT-PCR (n=6).

S6 Adropin$^{34-76}$ treatment did not affect IKK pathway in the liver.

The phosphorylation levels of Ser-176/180 in inhibitor-κB kinase α/β (IKKα/β) in whole tissue lysates (n=4-5) and the levels of nuclear factor κB p65 subunit (N-κB p65) in the nuclear extract (n=4-5) were determined by Western blotting. α-tubulin and histone H3 were used as the loading control in whole tissue lysates and nuclear lysates, respectively. The same α-tubulin band was used as the loading control for the blot of total IRS1 (Fig. 1A) and the blots of pAkt (S473) and total Akt (Fig. 2A). The same histone H3 band was used as the loading control for the blots of (n)FoxO1 (Fig. 2D), (n)SREBP1c (Fig. 6A) and (n)CRTC2 (Fig. 8B).

S7 Adropin$^{34-76}$ treatment did not affect the phosphorylation level of AMPK in the liver.

The phosphorylation levels of Thr-172 in AMP-activated protein kinase (AMPK) were determined by Western blotting (n=4-5). β-actin was used as the loading control.

S8 DIO mice displayed increased phosphorylation level of PKA substrate sites in IP3R in the liver.

The phosphorylation levels of PKA substrate sites in IP3R1 in DIO mice maintained on HF and lean mice on LF were measured by Western blotting following immunoprecipitation of IP3R1 (n=4). HF vs LF: **, $P<0.01$.